Journal of Theoretical Biology 264 (2010) 585–592

Contents lists available at ScienceDirect

Journal of Theoretical Biology

journal homepage: www.elsevier.com/locate/yjtbi

Helix–helix interactions and their impact on protein motifs and assemblies

Natalya Kurochkina *

Department of Biophysics, The School of Theoretical Modeling, P.O. Box 15676, Chevy Chase, MD 20825, USA

ARTICLE INFO

Article history:
Received 17 October 2009
Received in revised form
24 January 2010
Accepted 16 February 2010
Available online 2 March 2010

Keywords:
Helix interactions
Heptad repeat
Protein conformation
Structural motif
Protein assembly

ABSTRACT

Protein secondary structure elements are arranged in distinct structural motifs such as four-α-helix bundle, 8α/8β TIM-barrel, Rossmann dinucleotide binding fold, assembly of a helical rod. Each structural motif is characterized by a particular type of helix–helix interactions. A unique pattern of contacts is formed by interacting helices of the structural motif. In each type of fold, edges of the helix surface, which participate in the formation of helix–helix contacts with preceding and following helices, differ. This work shows that circular arrangements of the four, eight, and sixteen α-helices, which are found in the four-α-helical motif, TIM-barrel 8α/8β fold, and helical rod of $16.\bar{3}$ helices per turn correspondingly, can be associated with the mutual positioning of the edges of the helix surfaces. Edges $(i, i+1)-(i+1, i+2)$ of the helix surface are central for the interhelical contacts in a four-α-helix bundle. Edges $(i, i+1)-(i+2, i+3)$ are involved in the assembly of four-α-helix subunits into helical rod of a tobacco mosaic virus and a three-helix fragment of a Rossmann fold. In 8α/8β TIM-barrel fold, edges $(i, i+1)-(i+5, i+6)$ are involved in the octagon arrangement. Approximation of a cross section of each motif with a polygon (n-gon, $n=4, 8, 16$) shows that a good correlation exists between polygon interior angles and angles formed by the edges of helix surfaces.

1. Introduction

Protein tertiary structure exhibits many structural arrangements of regularly positioned secondary structure elements. These well characterized motifs such as four-α-helical bundle (Hendrickson et al., 1975), TIM-barrel 8α/8β fold (Alber et al., 1981), Rossmann fold (Rao and Rossmann, 1973) occur in a variety of proteins with diverse function.

The four-α-helical motif is found in hemerythrins (Sheriff et al., 1987), ferritins (Andrews et al., 1989), tobacco mosaic virus coat protein (Namba and Stubbs, 1986), cytochrome b_{562}, cytochrome c' (Mathews, 1985), transcription factors (Banner et al., 1987), membrane M2 proton channel of influenza A virus (Schnell and Chou, 2008; Pielak et al., 2009), and other proteins. This motif represents an arrangement of four α-helices that form interfaces in parallel or antiparallel manner (Review: Harris et al., 1994; Kohn et al., 1977). The four-α-helical structure also serves as a unit of higher assemblies. The subunit of a tobacco mosaic virus coat protein, which is a four-α-helix bundle, assembles in a helical rod wrapped around viral RNA. Three turns of the helical rod contain 49 subunits (Namba et al., 1989; Bhyravbhatla et al., 1998).

A TIM-barrel protein consists of eight-stranded β-barrel surrounded by eight parallel α-helices. This structural motif, first seen in triose phosphate isomerase (Alber et al., 1981), is also characteristic of a number of proteins: pyruvate kinase, malate synthase, and fructose-1, 6-bisphosphate, 2-keto-3-deoxy-6-phosphogluconate and D-2-deoxyribose-5-phosphate aldolases. Proteins of the Rossmann fold possess a topology of alternating α-helices and β-strands with βαβ ADP-binding structural unit characterized by a specific sequence pattern (Rao and Rossmann, 1973). They contain five, six, or seven parallel β-strands surrounded by α-helices, almost the same number of strands and helices as compared to TIM-barrel proteins. However, β-structure, being almost flat, is flanked by three or more α-helices on each side in contrast to circular arrangement of the TIM-barrel. This group is represented by lactate dehydrogenase, malate dehydrogenase, uridine-diphosphate galactose and uridine-diphosphate-N-acetylglucosamine 4-epimerases, pyridoxal phosphorylase B, glycosyltransferases, and other proteins. Numerous variants of the classic βαβ dinucleotide-binding (Rossmann) fold include nucleotide-binding domain and catalytic domain of the D-lactate dehydrogenase; the former is widely conserved among NAD-dependent dehydrogenases 6-stranded parallel β-sheet with α-helices packed on each side and GxGxxG sequence motif; the latter has a 5-stranded parallel β-sheet packed on each side by α-helices, which lacks a characteristic nucleotide-binding sequence motif. Comparison with L-lactate dehydrogenase shows deletion of the third β-strand and addition of one α-helix/β-strand pair to the N-terminus of the D-lactate dehydrogenase (Stoll, 1996).

* Tel.: +240 381 2383; fax: +202 508 3799.
E-mail address: info@schtm.org

0022-5193/$ - see front matter © 2010 Elsevier Ltd. All rights reserved.
doi:10.1016/j.jtbi.2010.02.026

The principles of helix–helix packing were described for the geometry of the interacting surfaces (Crick, 1953; Chothia et al., 1981; Efimov, 1979; Gernert et al., 1995) and energetics of the native, folded, and misfolded conformations including 4-α-helix packing (Chou et al., 1990), 8α/8β (Chou and Carlacci, 1991) and other types of associations. Amino acids at helix–helix interfaces influence the orientation of helices and interhelical angles (Kurochkina, 2007, 2008).

Secondary structure elements compose approximately 80% of the protein molecule and their interactions are considered as major contributors to the determination of a particular fold. Energetically favorable ways of packing secondary structure elements can be determined from conformational energy of noncovalent interactions (Chou et al., 1983, 1984, 1990; Carlacci and Chou, 1990b, 1991). Energetics of interactions of regular structural elements (Chou et al., 1990) and their packing arrangements including α-helix and β-sheet (Chou et al., 1985), two β-sheets (Chou et al., 1986), α-helices of the four-α-helix motif (Chou et al., 1988; Carlacci and Chou, 1990c; Carlacci et al., 1991), larger assemblies of the seven-helix bundle of bacteriorhodopsin (Chou et al., 1992a), and eight α-helices of myoglobin (Gerritsen et al., 1985) were extensively studied.

For non-polar and hydrogen-bonded polar atomic groups, important concepts of hydrophobic bond (Kauzmann, 1959) and accessible surface area (Richards, 1977; Lee and Richards, 1971) were introduced. Data obtained for protein unfolding and aqueous dissolution of hydrophobic model compounds were used to suggest principles of hydrophobic interactions (Privalov and Gill, 1988). Energy of hydrophobic interactions derived from the data on free energy of transfer of amino acid side chains from organic solvents to water was found to be proportional to accessible surface area for each amino acid side chain (Chothia, 1975). Contribution of all factors such as solvent, intermolecular bonds, entropy effects, has to be considered in order to correlate estimated and measured quantities (Chou, 1988).

Although interaction energy between the loops and loop–helix interaction of the four-helix structure was found to play a significant role in the stability of the structure (Carlacci and Chou, 1990a, 1990b, 1990c; Chou et al., 1992b) particularly for those molecules that possess long loops (Chou and Zheng, 1992), significance of core residues of the interacting secondary structure elements for the formation of a protein three-dimensional structure was demonstrated by ability of α-helices and β-sheets to associate as a pair of α-helices of GCN4 transcription factor (O'Shea et al., 1991), a dimer of two-helical fragments resulting in a four-helix motif of ROP protein (Paliakasis and Kokkinidis, 1991), an active recombinant Fv fragment of antibody after rearrangement of loops (Brinkmann et al., 1997).

In this work, the arrangement of contacts between α-helices in each of the structural motifs is addressed. There exists a relationship between the intrinsic properties of α-helix and the

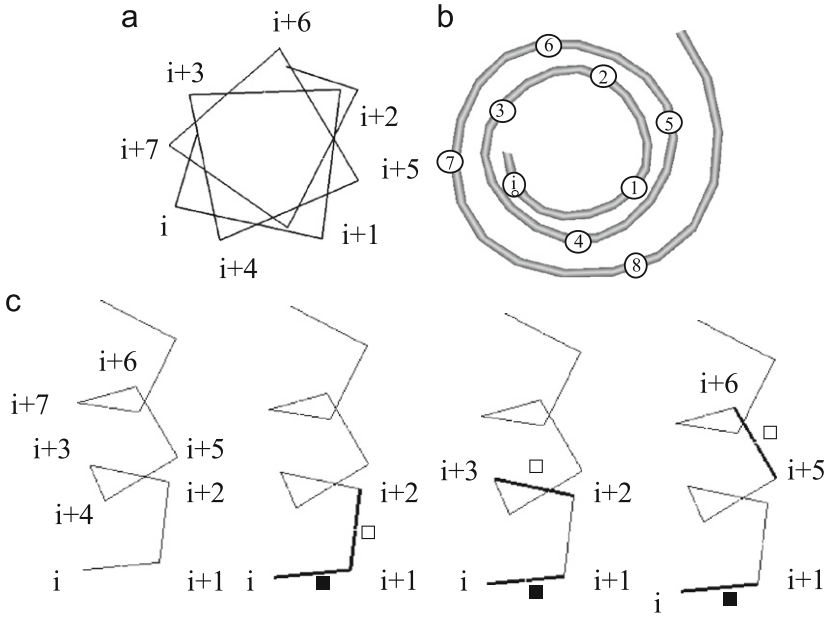

d

Edge 1	Edge 2	Average angle between planes containing edge1 and edge2	Interior angle of ideal n-gon 180°*(n-2)/n
(i, i+1)	(i+1, i+2)	100°±2.6	n=4, 90°
(i, i+1)	(i+2, i+3)	159°±2.8	n=16, 157°
(i, i+1)	(i+3, i+4)	60°±2.6	
(i, i+1)	(i+4, i+5)	41°±2.5	
(i, i+1)	(i+5, i+6)	140°±3.1	n=8, 135°
(i, i+1)	(i+6, i+7)	22°±2.2	

Fig. 1. α-Carbon backbone of α-helix. (a) Helical wheel. (b) "Wenxiang diagram", a conical projection suggested by Chou et al. (1997); a circled number gives a position of each amino acid relative to the first amino acid *i*. (c) Edges (thick line) of the α-helix (α-carbon backbone—thin line) participating in the formation of contacts with preceeding (■) or following (□) α-helix. (d) Angles between the planes containing corresponding edges.

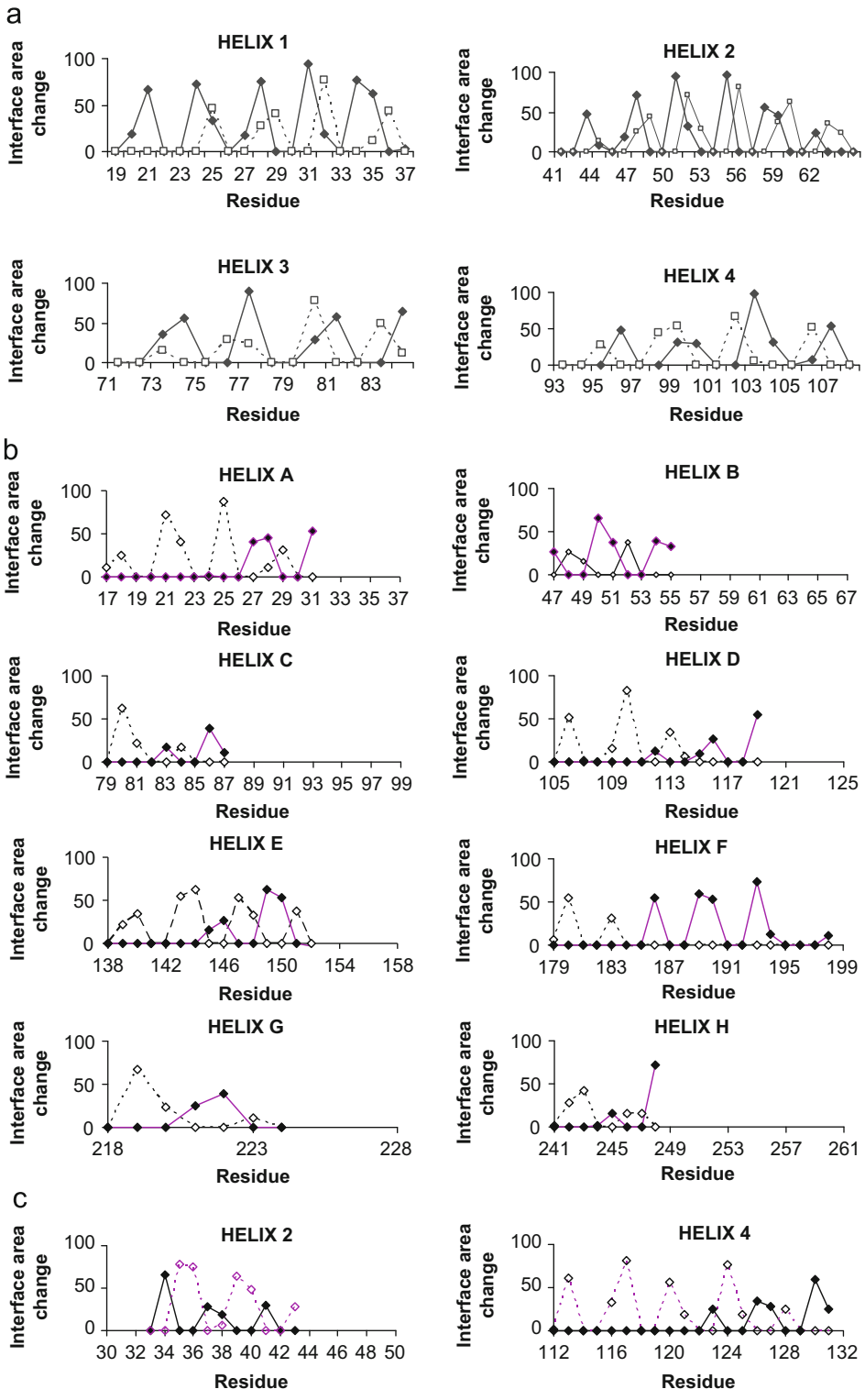

Fig. 2. Interface area change of amino acid residues of each helix observed in helix–helix interactions with preceding (■) or following (□) helix. (a) Myohemerythrin. (b) Triosephosphate isomerase. (c) L-lactate dehydrogenase.

types of tertiary structure motifs. It is shown that circular arrangements of the four, eight, and sixteen α-helices, which are found in four-α-helical motif, TIM-barrel 8α/8β fold, and helical rod of $16.\bar{3}$ helices per turn correspondingly, can be associated with the mutual positioning of the edges of helical surfaces. Edges $(i,\ i+1)-(i+1,\ i+2)$ of the helix surface are central for the interhelical contacts in a four-helix bundle. Edges $(i,\ i+1)-(i+2,\ i+3)$ are involved in the assembly of four-helix subunits into a helical rod of a tobacco mosaic virus and a three-helix fragment of a Rossmann fold. In an 8α/8β TIM-barrel fold, edges $(i,\ i+1)-(i+5,\ i+6)$ are involved in the octagon arrangement. Approximation of each motif with a polygon (n-gon, $n=4, 8, 16$) shows that a good correlation exists between the polygon interior angles and angles formed by the edges of the helix surfaces.

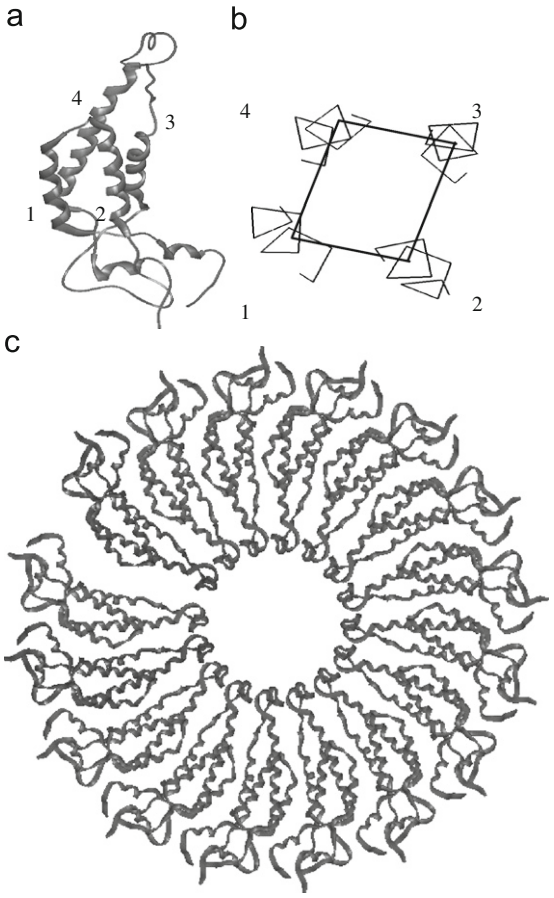

Fig. 3. Tobacco mosaic virus coat protein. (a) One four-α-helix subunit; helices 1–4. (b) Cross section of one four-α-helix subunit. (c) Assembly of the four-α-helix subunits into a helical rod—16.$\bar{3}$ subunits per one helical turn.

2. Results

In α-helix, one turn is made by 3.6 (in globular proteins) or 3.5 (in fibrous coiled coil proteins) amino acid residues (Fig. 1). The peptide group atoms C_α^i, C^i, N^{i+1}, C_α^{i+1}, and C_β^{i+1} are located between the two adjacent α-carbon atoms while side chains protrude to interact with side chains of the same helix and with the neighboring secondary structure elements or loops. On the surface of the helix, edges (i, i+1), (i, i+3), (i, i+4) can be seen as border "knobs" and "holes" of the interacting helices.

Contacts on the surface of the α-helix follow a regular pattern. It can be seen that amino acid residues at the interface of the two α-helices show heptad (3–4) periodic repeat similarly to a leucine zipper coiled coil. Interface area change was calculated for the pairs of the interacting helices (Fig. 2). For each residue of the helix, change of the interface area upon contact with another helix shows contribution of this residue to the formation of the interface. The interface area change of amino acid residues of each helix that is observed in helix–helix interactions with the preceding or following in amino acid sequence helix for myohemerythrin (Fig. 2a), triose phosphate isomerase (Fig. 2b), and L-lactate dehydrogenase (Fig. 2c) shows distinct pattern of contacts characteristic for the particular type of fold.

To address the question whether circular arrangements of the four, eight, and sixteen α-helices, which are present in the four-α-helical motif (Fig. 3a, b), TIM-barrel 8α/8β fold (Fig. 4), and helical rod of 16.$\bar{3}$ helices per turn (Fig. 3c) correspondingly, can be associated with the mutual positioning of the edges of the helix surfaces, the angles between helical edges were calculated and compared with the angles of the polygons formed at a cross section of each motif (Fig. 1b, c).

Angle θ was calculated between the two planes, one containing edge (i, i+1), another containing adjacent edge (i+1, i+2). In the four-helix bundle, if edge (i, i+1) is central for the contacts with the preceding α-helix then edge (i+1, i+2) is central for the contacts with the following α-helix. The average value of $\theta = 100^\circ \pm 2.6$ shows a good correlation with an angle of a cross section of the four helix bundle approximated by a quadrilateral (Fig. 1c). On a plane, this quadrilateral (square) would have an angle of 90°. In three-dimensional space, the vertices of a quadrilateral are located on a helix, which results in a larger angle between the edges.

Similarly, angle θ was calculated between the two planes, one containing edge (i, i+1), another containing edge (i+2, i+3) (Fig. 1b, c). The average value of the angle between these two planes $\theta = 159^\circ \pm 2.8$ is approximately the same as the value of an interior angle in a 16-gon (157°). In the assembly of the four-helix bundle subunits of a tobacco mosaic virus, these two edges are central for the circular arrangement of 49 subunits forming a 3-turn helix. As a result, 16.$\bar{3}$ subunits per one circular turn form a 16-gon. The value of the angle between the planes containing edges (i, i+1) and (i+2, i+3) is in a good agreement with the ideal angle of a cross section approximated by a 16-gon (Fig. 1c).

A cross section of the TIM-barrel eight α-helices is an octagon (Fig. 4b). The angle $\theta = 140^\circ \pm 3.1$ between the planes containing edges (i, i+1) and (i+5, i+6) is close in value to the interior angle of 135° in an ideal octagon (Fig. 1b, c).

Edges (i, i+1)−(i+1, i+2) of the helix surface are central for the interhelical contacts in a four-helix bundle. Edges (i, i+1)−(i+2, i+3) are involved in the assembly of four-helix subunits into helical rod of a tobacco mosaic virus and a three-helix fragment of a Rossmann fold. The 8α/8β TIM-barrel fold utilizes edges (i, i+1)−(i+5, i+6).

L-Lactate dehydrogenase (Fig. 5) contains a seven-stranded almost flat β-sheet flanked by three α-helices on each side. This arrangement of α-helices is different from 4-gon or 8-gon and is more similar to an arc of a 16-gon.

The work presented here shows that there exists a relationship between the intrinsic properties of α-helix and the types of tertiary structure motifs that involve helix–helix interactions. As a result, circular arrangements of the four, eight, and sixteen α-helices, which are found in the four-α-helical motif, TIM-barrel 8α/8β fold, and helical rod of 16.$\bar{3}$ helices per turn correspondingly, can be associated with the mutual positioning of the edges of the helix surfaces. An approximation of a cross section of each motif with a polygon (n-gon, n=4, 8, 16) shows that a good correlation exists between the polygon interior angles and the angles formed by the edges of the helix surfaces. Edges (i, i+1)−(i+1, i+2) of the helix surface are central for the interhelical contacts in a four-helix bundle. Edges (i, i+1)−(i+2, i+3) are involved in the assembly of four-helix subunits into helical rod of a tobacco mosaic virus and a three-helix fragment of a Rossmann fold. In 8α/8β TIM-barrel fold, edges (i, i+1)−(i+5, i+6) are involved in the octagon arrangement.

3. Methods

3.1. Angles between the planes containing edges of the helix surface

Two consecutive amino acids, amino acid i and amino acid i+1, form (i, i+1) edge on the surface of the helix (Fig. 1). Equation for the plane that contains the edge (i, i+1) and, therefore, peptide

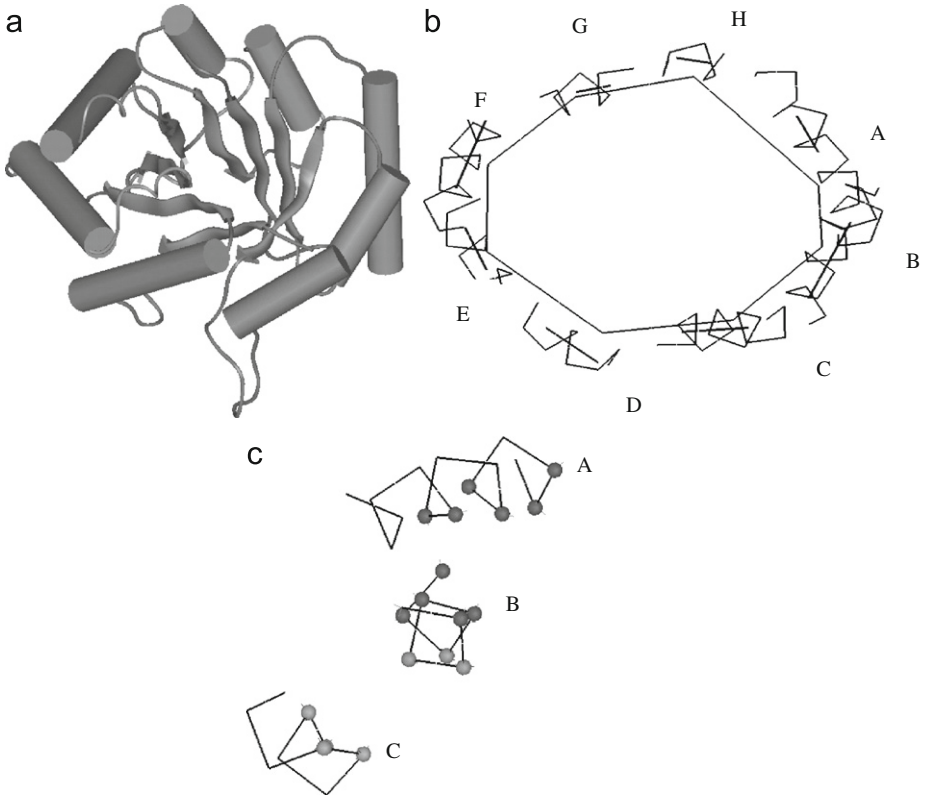

Fig. 4. Triose phosphate isomerase. (a) Three-dimensional structure (8α/8β: α-helices—cylinders, β-strands—ribbons). (b) Eight TIM-barrel helices named A–H of triose-phosphate isomerase approximated by an octagon with vertices at the center of mass of the interface residues in each helix. Helices (α-carbon backbone—thin line, axis—thick line) are directed so that their N-termini are below and their C-termini are beyond the plane of an octagon. The N-terminus to C-terminus vector of each helix points counterclockwise. (c) α-carbon atoms of the interface residues in helices A, B, and C (residues of AB interface—black spheres, residues of BC interface—grey spheres).

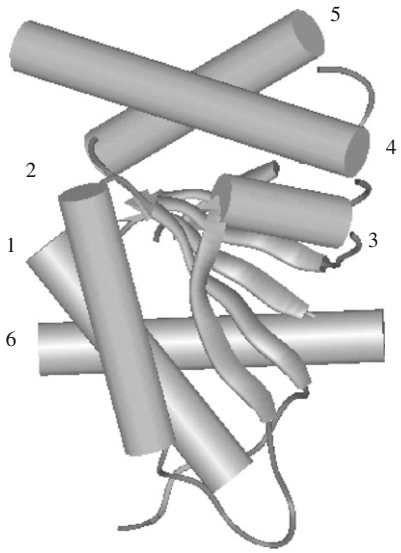

Fig. 5. L-lactate dehydrogenase. N-terminal domain (Rossman fold). A seven-stranded β-sheet (ribbons) flanked by α-helices (cylinders) 1, 2, and 6 on one side and α-helices 3, 4, and 5 on the opposite side.

group atoms C_α^i, C^i, N^{i+1}, C_α^{i+1}, and C_β^{i+1} can be written as

$$\begin{vmatrix} x & y & z \\ A_1 & A_2 & A_3 \\ B_1 & B_2 & B_3 \end{vmatrix} = 0,$$

where A_1, A_2, and A_3 are components of the vector C_α^i, C_α^{i+1}; B_1, B_2, and B_3 are components of the vector C_β^{i+1}, C_α^{i+1}, and

$$\begin{vmatrix} A_2 & A_3 \\ B_2 & B_3 \end{vmatrix}, \begin{vmatrix} A_1 & A_3 \\ B_1 & B_3 \end{vmatrix}, \text{ and } \begin{vmatrix} A_2 & A_3 \\ B_2 & B_3 \end{vmatrix}$$

are components of the normal vector N to this plane.

The angle θ between the two planes, one containing edge (i, i+1), another containing edge (i+1, i+2), is calculated as an angle between their normal vectors $N_1(x_1, y_1, z_1)$ and $N_2(x_2, y_2, z_2)$:

$$\theta = \cos^{-1}(x_1x_2 + y_1y_2 + z_1z_2) / \left(\sqrt{x_1^2 + y_1^2 + z_1^2} \times \sqrt{x_2^2 + y_2^2 + z_2^2} \right).$$

Similarly, angles for other pairs of planes of the helix surface are calculated (Fig. 1b). These angles are compared with the ideal interior angles of the n-sided polygon $\theta_{\text{ideal}} = 180^\circ(n-2)/n$.

3.2. The amount of area of the amino acid covered by contact with another helix

The amount of surface area that amino acid buries in contact with another α-helix was calculated as interface area change

$$(A_i - A_c) \times 100\%/A_i,$$

where A_i is the total solvent accessible area of the amino acid in isolated α-helix, i.e. α-helix taken from protein interior and placed into solvent; A_c is the solvent accessible area of amino acid when being in contact with another α-helix. Therefore, difference $A_i - A_c$ represents the amount of surface area covered by contact with another α-helix for each amino acid.

Table 1
Proteins of the four-α-helix, TIM-barrel, and Rossmann fold.

Protein	Source	PDB designation
Four-α-helix bundle		
Myohemerythrin	*Thermiste zostericola*	2 mhr
Hemerythrin	*Thermiste discrita*	2hmq
Coat protein	Tobacco mosaic virus	2tmv, 1ei7
Cytochrome b562	*Escherichia coli*	256b
Cytochrome c'	*Chromatium vinosum*	1bbh
Bacterioferritin	*Escherichia coli*	1bcf
Ferritin	*Homo sapiens*	1fha
TIM-barrel		
Triose phosphate isomerase	*Trypanosoma brucei*	5tim
	Leischmania mexicana	1n55
	Plasmodium falciparum	1o5x
	Saccharomyces cereviciae	7tim
Fructose-1,6-biphosphate aldolase	*Thermus aquaticus*	1rvg
	Drosophila melanogaster	1fba
	Homo sapiens	1ald
	Escherichia coli	2coa
	Orictolagus cuniculus	3vb4, 3dft
Enolase	*Trypanosoma brucei*	1oep
	Saccharomyces cereviciae	3enl
	Homo sapiens	1te6
Malate synthase	*Escherichia coli*	1p7t
	Mycobacterium tuberculosis	1n8w
Pyruvate kinase	*Orictolagus cuniculus*	1pkn
	Homo sapiens	1liu
Rossmann fold		
L-lactate dehydrogenase (L-LDH)	*Deinococcus radiodurans*	2v6b
	Champsocephalus gunnari	2v6b
	Thermus thermophilus	2v7b
	Saccharomyces cereviciae	2oz0
	Spaphylococcus aureus	3d4p
	Toxoplasma gondii	3czm
	Squalus acanthias	6ldh
D-lactate dehydrogenase (D-LDH)	*Lactobacillus helveticus*	2dld
Malate dehydrogenase (MDH)	*Sus scrofa*	1mld
	Aeropyrum pernix	2d4a
	Entamoeba hystolitica	3i0p
Uridine-diphosphate-galactose 4-epimerase	*Trypanosoma brucei*	1gy8
Uridine-diphosphate-N-acetylglucosamine 4-epimerase	*Pseudomonas aeruginosa*	1sb8
Pyridoxal phosphorylase B	*Oryctolagus cuniculus*	1skc

3.3. Protein data set

Proteins, which contain the four-helix bundle, TIM-barrel and Rossmann folds are listed in Table 1. The accessible surface area change was calculated for the helices 1–4 of myohemerythrin, helices A–H of triose-phosphate isomerase, and helices 1–6 of the L-lactate dehydrogenase (Table 2).

Protein crystallographic structures were used from the Protein Data Bank (PDB) (Bernstein et al., 1977).

4. Discussion

The work reported here shows that there exists a relationship between the intrinsic properties of α-helix and the types of tertiary structure motifs formed by the interacting α-helices such as circular arrangements of the four, eight, and sixteen α-helices.

These results indicate that there are several possible arrangements of α-helices, which originate from structural properties of the interacting helix surfaces. There are many enzymes, which possess the same structure, for instance, of TIM-barrel motif. The function of each enzyme differs, but common shape of the motif is conserved, particularly when these proteins bind the same or similar ligands. Similarly, the main structural unit βαβ of a Rossman fold is a dinucleotide binding motif. Although there are examples of protein families that possess similar tertiary structure without exhibiting preferences for the common ligands such as globins, phycocyanins and toxins, it has been proposed that these shared architectural features may be a trace of a distant evolutionary relationship (Holm and Sander, 1993).

Ability of secondary structure elements to associate in different forms gives rise to various shapes of assemblies. Tobacco mosaic virus is assembled in a helical rod carrying viral RNA

Table 2
Amino acid residues that form α-helices in myohemerythrin (four-α-helix), triose phosphate isomerase (TIM-barrel), and L-lactate dehydrogenase (Rossmann fold).

Protein	Source	Pdb code	Amino acid residues of a-helices	Helix name
Myohemerythrin	*Thermiste zostericola*	2mhr	19–37	1
			41–64	2
			71–84	3
			93–108	4
Triose phosphate isomerase	*Leishmania mexicana*	1n55	17–31	A
			47–55	B
			79–87	C
			105–119	D
			138–152	E
			179–198	F
			218–224	G
			241–248	H
L-Lactate dehydrogenase	*Deinococcus radiodurans*	2v6b	30–43	1
			55–67	2
			84–89	3
			112–131	4
			141–153	5
			247–263	6

inside. Bacterioferritin subunits are shaped as a spherical shell, storage of iron (Frolow et al., 1994). Morphological features can be considered in a more detailed way with respect to structurally justified arrangements.

Crystal growth is dependent to a large extent on satisfying strict requirements of the lattice contacts. Existence of a limited number of helix arrangement patterns when applied to the analysis of crystal packing may contribute to understanding of this complex process. It also raises a question as to whether similar structural relationships will be found in other types of packing of secondary structure elements.

References

Alber, T., Banner, D.W., Bloomer, A.C., Petsko, G.A., Phillips, D., Rivers, P.S., Wilson, I.A., 1981. On the three-dimensional structure and catalytic mechanism of triose phosphate isomerase. Philos. Trans. R. Soc. London 293, 159–171.

Andrews, C.A., Smith, J.A.A., Guest, J.R., Harrison, P.M., 1989. Amino acid sequence of the bacterioferritin (cytochrome b_1) of *Escherichia coli*-K12. Biochem. Biophys. Res. Commun. 158, 489–496.

Banner, D.W., Kokkinidis, M., Tsernoglou, D., 1987. Structure of the ColE1 Rop protein at 1.7 Å resolution. J. Mol. Biol. 196, 657–675.

Bernstein, F.C., Koetzle, T.F., Williams, G.J.B., Meyer Jr., E.F., Brice, M.D., Rodgers, J.R., Kennard, O., Shimanouchi, T., Tasumi, M., 1977. The protein data bank: a computer-based archival file for macromolecular structures. J. Mol. Biol. 112, 535–542.

Bhyravbhatla, B., Watowich, S.J., Caspar, D.L., 1998. Refined atomic model of the four-layer aggregate of the tobacco mosaic virus coat protein at 2.4-A resolution. Biophys. J. 74, 604–615.

Brinkmann, U., Di Carlo, A., Vasmatzis, G., Kurochkina, N., Beers, R., Lee, B., Pastan, I., 1997. Stabilization of a recombinant Fv fragment by base loop interconnection and VH-VL permutation. J. Mol. Biol. 268, 107–117.

Carlacci, L., Chou, K.C., 1990a. Electrostatic interactions between loops and α-helices in four-helix bundle proteins. Protein Eng. 4, 225–227.

Carlacci, L., Chou, K.C., 1990b. Monte Carlo method applied in the search for low energy conformations of ßaßaß structures. Biopolymers 30, 135–150.

Carlacci, L., Chou, K.C., 1990c. Energetic approach to the folding of four α-helices connected sequentially. Protein Eng. 3, 509–514.

Carlacci, L., Chou, K.C., 1991. New development on energetic approach to the packing in proteins. J. Comput. Chem. 12, 410–415.

Carlacci, L., Chou, K.C., Maggiora, G.M., 1991. A heuristic approach to predicting the tertiary structure of bovine somatotropin. Biochemistry 30, 4389–4398.

Chothia, C., 1975. Structural invariants in protein folding. Nature 254, 304–308.

Chothia, C., Levitt, M., Richardson, D., 1981. Helix to helix packing in proteins. J. Mol. Biol. 145, 215–250.

Chou, K.C., 1988. Review: low-frequency collective motion in biomacromolecules and its biological functions. Biophys. Chem. 30, 3–48.

Chou, K.C., Carlacci, L., 1991. Energetic approach to the folding of alpha/beta barrels. Proteins 9, 280–293.

Chou, K.C., Carlacci, L., Maggiora, G.M., Parodi, L.A., Schultz, M.W., 1992a. An energy-based approach to packing the 7-helix bundle of bacteriorhodopsin. Protein Sci. 1, 810–827.

Chou, K.C., Maggiora, G.M., Nemethy, G., Scheraga, H.A., 1988. Energetics of the structure of the four-alpha-helix bundle in proteins. Proc. Natl. Acad. Sci. USA 85, 4295–4299.

Chou, K.C., Maggiora, G.M., Scheraga, H.A., 1992b. The role of loop–helix interactions in stabilizing four-helix bundle proteins. Proc. Natl. Acad. Sci. USA 89, 7315–7319.

Chou, K.C., Nemethy, G., Rumsey, S., Tuttle, R.W., Scheraga, H.A., 1985. Interactions between an alpha-helix and a beta-sheet: energetics of alpha/beta packing in proteins. J. Mol. Biol. 186, 591–609.

Chou, K.C., Nemethy, G., Scheraga, H.A., 1983. Energetic approach to packing of α-helices: 1. Equivalent helices. J. Phys. Chem. 87, 2869–2881.

Chou, K.C., Nemethy, G., Scheraga, H.A., 1984. Energetic approach to packing of α-helices: 2. General treatment of nonequivalent and nonregular helices. J. Am. Chem. Soc. 106, 3161–3170.

Chou, K.C., Nemethy, G., Scheraga, H.A., 1990. Review: energetics of interactions of regular structural elements in proteins. Acc. Chem. Res. 23, 134–141.

Chou, K.C., Nemethy, G., Rumsey, S., Tuttle, R.W., Scheraga, H.A., 1986. Interactions between two beta-sheets: energetics of beta/beta packing in proteins. J. Mol. Biol. 188, 641–649.

Chou, K.C., Zhang, C.T., Maggiora, G.M., 1997. Disposition of amphiphilic helices in heteropolar environments. Proteins: Struct. Funct. Genet. 28, 99–108.

Chou, K.C., Zheng, C., 1992. Strong electrostatic loop–helix interactions in bundle motif protein structures. Biophys. J. 63, 682–688.

Crick, F., 1953. Acta Crystallogr. 6, 689.

Efimov, A., 1979. Packing of α-helices in globular proteins. Layer structure of globin hydrophobic cores. J. Mol. Biol. 134, 23–40.

Frolow, F., Kalb (Gilboa), A.J., Yariv, J., 1994. The structure of a unique two-fold symmetric, haem-binding site. Nat. Struct. Biol. 1, 453–460.

Gernert, K.M., Surles, M.C., Labean, T.H., Richardson, J.S., Richrdson, D.C., 1995. The alacoil: a very tight, antiparallel coiled-coil of helices. Protein Sci. 4, 2252–2260.

Gerritsen, M., Chou, K.C., Nemethy, G., Scheraga, H.A., 1985. Energetics of multi-helix interactions in protein folding: application to myoglobin. Biopolymers 24, 1271–1293.

Harris, N.L., Presnell, S.R., Cohen, F.E., 1994. Four helix bundle diversity in proteins. J. Mol. Biol. 236, 1356–1368.

Hendrickson, W.A., Klippenstein, G.L., Ward, K.B., 1975. Tertiary structure of myohemerythrin at low resolution. Proc. Natl. Acad. Sci. 72, 2160–2164.

Holm, L., Sander, C., 1993. Structural alignment of globins, phycocyanins and colicin A. FEBS Lett. 315, 301–306.

Kauzmann, W., 1959. Some factors in the interpretation of protein denaturation. Adv. Protein Chem. 14, 1–63.

Kohn, W.D., Mant, C.T., Hodges, R.S., 1977. α-helical protein assembly motifs. J. Biol. Chem. 272, 2583–2586.

Kurochkina, N., 2007. Amino acid composition of parallel helix–helix interfaces. J. Theor. Biol. 247, 110–121.

Kurochkina, N., 2008. Specific sequence combinations at parallel and antiparallel helix–helix interfaces. J. Theor. Biol. 255, 188–198.

Lee, B., Richards, F.M., 1971. The interpretation of protein structures: estimation of static accessibility. J. Mol. Biol. 55, 379–400.

Mathews, F.S., 1985. The structure, function, and evolution of cytochromes. Prog. Biophys. Mol. Biol. 45, 1–56.

Namba, K., Stubbs, G., 1986. Structure of tobacco mosaic virus at 3.6 Angstroms resolution. Implications for assembly. Science 231, 1401–1406.

Namba, K., Pattanayek, R., Stubbs, G., 1989. Visualization of protein–nucleic acid interactions in a virus. Structure of intact tobacco mosaic virus at 2.9 Angstrom resolution by X-ray fiber diffraction. J. Mol. Biol. 208, 307–325.

O'Shea, E.K., Klemm, J.D., Kim, P.S., Alber, T., 1991. Crystal structure of GCN4 leucine zipper, a two-stranded parallel coiled coil. Science 254, 539–544.

Paliakasis, C.D., Kokkinidis, M., 1991. The stability of the four-α-helix bundle motif in proteins. Protein Eng. 4, 849–850.

Pielak, R.M., Jason, R., Schnell, J.R., Chou, J.J., 2009. Mechanism of drug inhibition and drug resistance of influenza A M2 channel. Proc. Natl. Acad. Sci. USA 106, 7379–7384.

Privalov, P.L., Gill, S.J., 1988. Stability of protein structure and hydrophobic interaction. Adv. Protein Chem. 39, 191–234.

Rao, S.T., Rossmann, M.G., 1973. Comparison of super-secondary structure in proteins. J. Mol. Biol. 76, 241–256.

Richards, F.M., 1977. Areas, volumes, packing, and protein structure. Annu. Rev. Biophys. Bioeng. 6, 151–176.

Schnell, J.R., Chou, J.J., 2008. Structure and mechanism of the M2 proton channel of influenza A virus. Nature 451, 591–595.

Sheriff, S., Hendrickson, W.A., Smith, J.L., 1987. Structure of myohemerythrin in the azidomet state at 1.7/1.3 Å resolution. J. Mol. Biol. 197, 273–296.

Stoll, V.S., 1996. Insights into substrate binding by D-2-ketoacid dehydrogenases from the structure of *Lactobacillus pentosus* D-lactate dehydrogenase. Structure 4, 437–447.